

## Soffer's inequality and the transversely polarized Drell-Yan process at next-to-leading order

O. Martin,<sup>1</sup> A. Schäfer,<sup>1</sup> M. Stratmann,<sup>2,\*</sup> and W. Vogelsang<sup>3</sup>

<sup>1</sup>*Institut für Theoretische Physik, Universität Regensburg, D-93040 Regensburg, Germany*

<sup>2</sup>*Institut für Physik, Universität Dortmund, D-44221 Dortmund, Germany*

<sup>3</sup>*Theory Division, CERN, CH-1211 Geneva 23, Switzerland*

(Received 9 October 1997; published 10 February 1998)

We check numerically if Soffer's inequality for quark distributions is preserved by next-to-leading order QCD evolution. Assuming that the inequality is saturated at a low hadronic scale, we estimate the maximal transverse double-spin asymmetry for Drell-Yan muon pair production to next-to-leading-order accuracy. [S0556-2821(98)05005-X]

PACS number(s): 13.88.+e, 12.38.Bx

### I. INTRODUCTION

The transversity distribution  $\delta q(x, Q^2)$  is the only completely unknown twist-2 parton distribution function of the nucleon. In a transversely polarized nucleon it counts the number of quarks with spin parallel to the nucleon spin minus the number of quarks with antialigned spin [1]. In field theory the transversity distribution is defined by the expectation value of a chiral-odd operator between nucleon states, which is the reason why it is not experimentally accessible in inclusive deep inelastic lepton-nucleon scattering (DIS) [2,3]. The most promising hard process allowed by this chirality selection rule seems to be Drell-Yan dimuon production, and exactly this reaction will be utilized for attempting a first measurement of  $\delta q(x, Q^2)$  at the BNL Relativistic Heavy Ion Collider (RHIC) [4]. What actually will be measured is not the transversity distribution itself, but the transverse double-spin asymmetry  $A_{TT} = d\delta\sigma/d\sigma$ , where the polarized and unpolarized hadronic cross sections are defined as

$$d\delta\sigma \equiv \frac{1}{2}(d\sigma^{\uparrow\uparrow} - d\sigma^{\uparrow\downarrow}), \quad d\sigma \equiv \frac{1}{2}(d\sigma^{\uparrow\uparrow} + d\sigma^{\uparrow\downarrow}). \quad (1)$$

In perturbative QCD (PQCD)  $A_{TT}$  can be expressed in terms of unpolarized parton distributions, the yet unknown transversity distributions, and the relevant partonic cross sections. Although the latter have been known to next-to-leading-order (NLO) accuracy in the strong coupling for several years by now [5–7], consistent NLO calculations were not possible because of the lack of the two-loop transversity splitting functions. This situation changed only very recently [8–10], allowing for the first time a consistent calculation of PQCD corrections to the transverse double-spin asymmetry for the Drell-Yan process.

The unpolarized, longitudinally and transversely polarized quark distributions ( $q$ ,  $\Delta q$ ,  $\delta q$ ) of the nucleon are expected to obey the rather interesting relation

$$2|\delta q(x)| \leq q(x) + \Delta q(x) \quad (2)$$

derived by Soffer [11]. It has been recently clarified that Soffer's inequality is preserved by leading-order (LO) QCD evolution, i.e., if Eq. (2) is valid at some scale  $Q_0$ , it will also be valid at  $Q > Q_0$  [12]. To NLO the situation is not as simple. The parton distributions are now subject to the choice of the factorization scheme which one may fix independently for  $q$ ,  $\Delta q$ , and  $\delta q$ . One can therefore always find "sufficiently incompatible" schemes in which a violation of Eq. (2) occurs. However, in Ref. [8] it was shown with analytical methods that the inequation for valence densities is preserved by NLO QCD evolution in a certain "Drell-Yan scheme" in which the NLO cross sections for dimuon production maintain their LO forms, and also in the modified minimal subtraction ( $\overline{\text{MS}}$ ) scheme. An analytical check of the sea part is difficult since the singlet mixing between quarks and gluons has to be taken into account for the unpolarized and longitudinally polarized quantities on the right-hand-side (RHS) of Eq. (2). In Sec. II of this article we shall show numerically that Soffer's inequation for sea quarks is also preserved under NLO evolution.

Estimates of  $A_{TT}$  suffer of course from the fact that no experimental information on the transversity distribution is available at the moment. Therefore one has to rely on ansätze or model calculations of  $\delta q(x, Q^2)$  at some reference scale  $Q_0$  [13]. For example, a popular assumption is  $\delta q(x, Q_0^2) = \Delta q(x, Q_0^2)$  which, however, is in general incompatible with Soffer's inequality (2), in particular in a situation in which  $\Delta q(x, Q_0^2) \approx -q(x, Q_0^2)$ . Our aim in Secs. III and IV will be to estimate within LO and NLO an upper bound on the transverse double-spin asymmetry for the Drell-Yan process. To do so, we will first of all assume the validity of Soffer's inequality, which seems reasonable and is corroborated by our finding of Sec. II that the NLO evolution to  $Q^2 > Q_0^2$  preserves the inequation once it is satisfied at the input scale. The maximal asymmetry  $A_{TT}$  can then be estimated by further assuming *saturation* of the Soffer bound (2). The result obtained for  $A_{TT}$  under this assumption obviously strongly depends on the value chosen for  $Q_0$ . If  $Q_0$  is taken to be large, i.e., of the order of the invariant mass  $M$  of the lepton pair which sets the typical hard scale for the Drell-Yan process, the largest possible values for  $A_{TT}$  will be reached. However, for several reasons it does not seem convincing to assume saturation of Eq. (2) by the input distribu-

\*Present address: Department of Physics, University of Durham, Durham, DH1 3LE, England.

tions employing such a high  $Q_0^2 \sim M^2$ : Firstly, evolving backwards to  $Q^2 < Q_0^2$  — which should be a completely legitimate procedure if  $Q_0$  is not small — will under such circumstances immediately yield a violation of Soffer's inequality. Second, the RHS of Eq. (2) will almost certainly lead to an overestimation for the  $\delta q$  if saturation is assumed at a large  $Q_0$ . For instance, for sea quarks the first moment ( $x$  integral) of the RHS of Eq. (2) will diverge, which is not expected for the integral over  $\delta \bar{q}$  at any  $Q^2$ . Therefore, to obtain a realistic estimate for an upper bound on  $A_{TT}$  by assuming saturation of Soffer's inequation, two requirements have to be met: (i) The saturation should be adopted only at a rather low ‘‘hadronic’’ input scale where (ii) the integral over the RHS of (2) is finite. Both demands are automatically satisfied if we choose the unpolarized and longitudinally polarized input parton distributions of the radiative parton model analyses [14–16] and set<sup>1</sup>

$$2\delta q(x, Q_0^2) = q(x, Q_0^2) + \Delta q(x, Q_0^2), \quad (3)$$

where  $Q_0$  now is identified with the input scale  $\mu \sim \mathcal{O}(0.6 \text{ GeV})$  of the radiative parton model [14], and is considered the smallest scale from which perturbative evolution can be performed, such that no backward evolution from  $\mu$  makes sense. While we are aware that our approach, with its rather small  $Q_0$ , may lead to an underestimation of the maximally possible  $A_{TT}$ , we still believe our results to be built on a firm basis, given the large phenomenological success [15,16] of the radiative parton model for the  $q$ ,  $\Delta q$ . In any case, our results for  $A_{TT}$  under the assumption of Eq. (3) are the largest the radiative parton model can predict, and will provide a useful target for future experiments. We emphasize that our NLO results presented in Sec. IV are, to our knowledge, the first ones to be obtained to true and consistent NLO accuracy. Section IV will also provide a discussion of other possible uncertainties of our results.

In Sec. V we will present our conclusions.

## II. PRESERVATION OF SOFFER'S INEQUATION BY NLO EVOLUTION

Unlike the case of the more familiar unpolarized and longitudinally polarized densities, all transversity distributions obey simple non-singlet-type evolution equations because there is no corresponding gluonic quantity due to angular momentum conservation [17,3]. Introducing

$$\delta q_{\pm}(x, Q^2) \equiv \delta q(x, Q^2) \pm \delta \bar{q}(x, Q^2), \quad (4)$$

and Mellin moments  $\delta q_{\pm}^n(Q^2) \equiv \int_0^1 dx x^{n-1} \delta q_{\pm}(x, Q^2)$ , the evolution equations are given by [5]

$$Q^2 \frac{d}{dQ^2} \delta q_{\pm}^n(Q^2) = \delta P_{qq, \pm}^n(\alpha_s(Q^2)) \delta q_{\pm}^n(Q^2). \quad (5)$$

The Mellin moments of the transverse splitting functions  $\delta P_{qq, \pm}^n$  are taken to have the following perturbative expansion:

$$\delta P_{qq, \pm}^n(\alpha_s) = \left( \frac{\alpha_s}{2\pi} \right) \delta P_{qq}^{(0), n} + \left( \frac{\alpha_s}{2\pi} \right)^2 \delta P_{qq, \pm}^{(1), n} + \dots, \quad (6)$$

i.e., both are equal to LO. We use the following NLO expression for the strong-coupling constant:

$$\frac{\alpha_s(Q^2)}{2\pi} = \frac{2}{\beta_0 \ln Q^2 / \Lambda^2} \left( 1 - \frac{\beta_1}{\beta_0^2} \frac{\ln \ln Q^2 / \Lambda^2}{\ln Q^2 / \Lambda^2} \right), \quad (7)$$

where  $\Lambda$  is the QCD scale parameter and  $\beta_0 = 11 - 2n_f/3$  and  $\beta_1 = 102 - 38n_f/3$ , with  $n_f$  being the number of active flavors. The solution of Eq. (5) is then simply given by [5]

$$\begin{aligned} \delta q_{\pm}^n(Q^2) = & \left[ 1 + \frac{\alpha_s(Q_0^2) - \alpha_s(Q^2)}{\pi \beta_0} \left( \delta P_{qq, \pm}^{(1), n} - \frac{\beta_1}{2\beta_0} \delta P_{qq}^{(0), n} \right) \right] \\ & \times \left( \frac{\alpha_s(Q^2)}{\alpha_s(Q_0^2)} \right)^{-2\delta P_{qq}^{(0), n} / \beta_0} \delta q_{\pm}^n(Q_0^2). \end{aligned} \quad (8)$$

Needless to say, the LO evolutions are entailed in the above equations when we set the NLO quantities  $\delta P_{qq, \pm}^{(1), n}$ ,  $\beta_1$  to zero.

Equation (8) can be very conveniently employed for a numerical calculation of the NLO evolution of the transversity distributions. As discussed in Sec. I, we will assume saturation of Soffer's inequality at the input scale; see Eq. (3). Our choice for the RHS of Eq. (3) will then be the NLO MS radiative parton model inputs for  $q(x, Q_0^2)$  of Ref. [15] and for the longitudinally polarized  $\Delta q(x, Q_0^2)$  of the ‘‘standard’’ scenario of Ref. [16] at  $^2 Q_0^2 = \mu_{\text{NLO}}^2 = 0.34 \text{ GeV}^2$ . For simplicity we will slightly deviate from the actual  $q(x, Q_0^2)$  of [15] in so far as we will neglect the breaking of SU(2) in the input sea quark distributions originally present in this set. This seems reasonable as SU(2) symmetry was also assumed for the  $\Delta \bar{q}(x, Q_0^2)$  of Ref. [16], which in that case was due to the fact that in the longitudinally polarized case there are no data yet that could discriminate between  $\Delta \bar{u}$  and  $\Delta \bar{d}$ . We therefore prefer also to assume  $\delta \bar{u}(x, Q_0^2) = \delta \bar{d}(x, Q_0^2)$  for the transversity input. We will examine the possible effects of SU(2) breaking later. The moments of the resulting input distributions  $\delta q(x, Q_0^2)$  are easily taken, and the  $\delta q_{\pm}^n(Q_0^2)$  are then evolved to higher scales  $Q^2 > Q_0^2$  with the help of Eq. (8). A standard inverse Mellin transformation finally gives the desired transversity distribution in  $x$  space. In order to perform this inverse Mellin transformation, Eq. (8) has to be analytically continued to complex  $n$  [14]. The evolutions of the  $q(x, Q_0^2)$  [neglecting the SU(2) breaking] and the

<sup>1</sup>The possibility of choosing a different sign in front of the right-hand side of Eq. (3) will be discussed later.

<sup>2</sup>Note that for the purpose of checking the preservation of Soffer's inequality by evolution the choice of the initial scale  $Q_0^2$  is actually irrelevant.

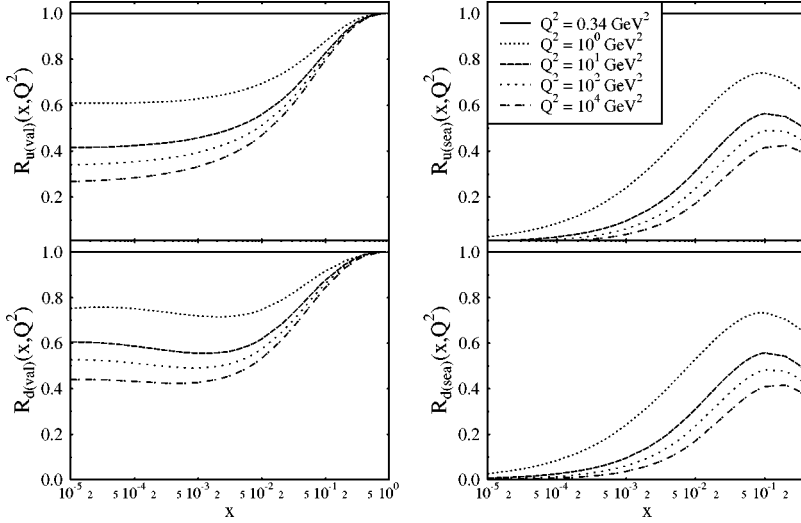


FIG. 1. The ratio  $R_q(x, Q^2)$  as defined in Eq. (9) for  $q = u_v, \bar{u}, d_v,$  and  $\bar{d}$ , and several fixed values of  $Q^2$ .

$\Delta q(x, Q_0^2)$ , which both involve the singlet mixing between quarks and gluons, proceed as explained in Refs. [14–16].

In order to numerically check the preservation of Eq. (2), Fig. 1 shows the ratio

$$R_q(x, Q^2) = \frac{2|\delta q(x, Q^2)|}{q(x, Q^2) + \Delta q(x, Q^2)} \quad (9)$$

as a function of  $x$  for several different  $Q^2$  values for  $q = u_v = u_-, \bar{u} = (u_+ - u_-)/2, d_v = d_-,$  and  $\bar{d} = (d_+ - d_-)/2$  [cf. Eq. (4)]. If NLO evolution preserves Soffer's inequality, then  $R_q(x, Q^2)$  should not become larger than 1 for any  $Q^2 \geq Q_0^2$ . As we already know from Ref. [8], this is the case for the two valence distributions. Figure 1 confirms that Soffer's inequality is indeed also preserved for sea distributions. Furthermore, in Fig. 1 we see that evolution leads to a strong suppression of  $R_q(x, Q^2)$  at small values of  $x$ , in particular for the sea quarks. This can be understood by the fact that  $\delta P_{qq, \pm}(x)$  has a very mild behavior for  $x \rightarrow 0$  [8], and by the well-known sharp small- $x$  rise of the unpolarized sea distributions in the denominator of  $R_q$  due to  $Q^2$  evolution. We note that our numerical results for the sea quarks became somewhat unstable at large  $x$ , probably caused by the fact that the sea distributions are obtained here as differences of two much larger quantities.

As is obvious from Eq. (2), Soffer's inequality only restricts the absolute value of the transversity distribution. Therefore, we are free to choose a different sign in front of the RHS of Eq. (3), and have to check the results for the two distinct possibilities  $\delta q_v(x, Q_0^2) > 0, \delta \bar{q}(x, Q_0^2) > 0$  and  $\delta q_v(x, Q_0^2) > 0, \delta \bar{q}(x, Q_0^2) < 0$ . Our results do not noticeably depend on the actual choice.

As we have neglected any possible SU(2) breaking in all the sea input distributions  $\bar{q}(x, Q_0^2), \Delta \bar{q}(x, Q_0^2),$  and  $\delta \bar{q}(x, Q_0^2)$ , any difference between the curves for  $R_{\bar{u}}$ , and  $R_{\bar{d}}$  can necessarily only result from the dynamical breaking of SU(2) first induced by NLO evolution. The occurrence of a small breaking from this source is well known from the unpolarized [18] and longitudinally polarized [19] cases. For the transversity densities it is given by

$$2(\delta \bar{u} - \delta \bar{d})^n(Q^2) = \frac{[\alpha_s(Q^2) - \alpha_s(Q_0^2)]}{\pi \beta_0} (\delta P_{qq, -}^{(1), n} - \delta P_{qq, +}^{(1), n}) \times \left( \frac{\alpha_s(Q^2)}{\alpha_s(Q_0^2)} \right)^{-2 \delta P_{qq}^{(0), n} / \beta_0} \times (\delta u_v - \delta d_v)^n(Q_0^2). \quad (10)$$

Figure 2 displays the resulting effect via the ratio

$$\delta D(x, Q^2) = \frac{\delta \bar{u}(x, Q^2) - \delta \bar{d}(x, Q^2)}{\delta \bar{u}(x, Q^2) + \delta \bar{d}(x, Q^2)} \quad (11)$$

for various  $Q^2$ . One can see that — apart from the region of very large  $x$  — the dynamical breaking of SU(2) is rather small, and could in reality well be entirely masked by the explicit breaking in the nonperturbative sea input.

### III. UPPER BOUNDS ON $A_{TT}$ : FRAMEWORK

Now that we have shown that NLO evolution preserves Soffer's inequation, we want to utilize it to derive upper

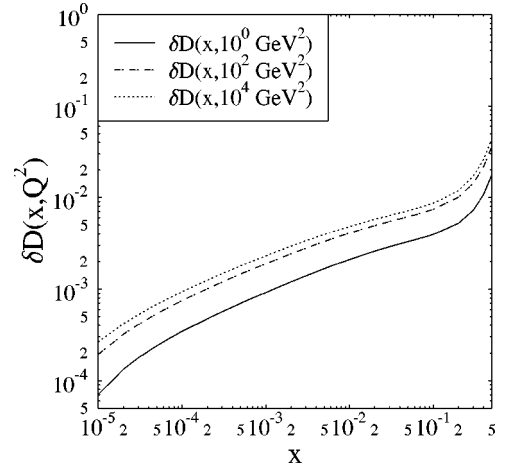


FIG. 2. The dynamical SU(2) breaking in the NLO transversity densities expressed by the ratio  $\delta D(x, Q^2)$  as defined in Eq. (11) for several fixed values of  $Q^2$ .

bounds on the transverse double-spin asymmetry to be measured in polarized Drell-Yan muon pair production. For this purpose we choose again the maximally allowed value (3) for the transversity distributions, which should yield the maximal double-spin asymmetry. We employ the same unpolarized and longitudinally polarized input distributions as in Sec. II, along with the same value for the initial scale  $Q_0$ .

The scaling variable for the Drell-Yan process is  $\tau = M^2/S$ , where  $M$  is the invariant mass of the produced muon pair and  $\sqrt{S}$  is the center-of-mass energy of the hadronic collision. Since in unpolarized reactions only the collision axis is specified, the distribution of the produced muon pairs cannot depend on the azimuth  $\phi$ . If the colliding nucleons are transversely polarized, then the collision and spin axes specify a plane in space and consequently the polarized cross section will depend on  $\phi$ . Instead of working with  $\tau$ -dependent cross sections, we again prefer Mellin moments defined by

$$\frac{d(\delta)\sigma^n}{d\phi} \equiv \int_0^1 d\tau \tau^{n-1} \frac{\tau d(\delta)\sigma}{d\tau d\phi}. \quad (12)$$

Including NLO corrections to these cross sections, one obtains the generic expression [6,7]

$$\begin{aligned} \frac{d(\delta)\sigma^n}{d\phi} &= \frac{\alpha_{em}^2}{9S} (\delta)\Phi(\phi) \left[ (\delta)H_q^n(Q_F^2) \right. \\ &\quad \times \left( 1 + \frac{\alpha_s(Q_R^2)}{2\pi} (\delta)C_q^{DY,n}(Q_F^2) \right) \\ &\quad \left. + H_g^n(Q_F^2) \frac{\alpha_s(Q_R^2)}{2\pi} (\delta)C_g^{DY,n}(Q_F^2) \right], \quad (13) \end{aligned}$$

where

$$(\delta)H_q^n(Q_F^2) \equiv \sum_q e_q^2 [(\delta)q_A^n(Q_F^2)(\delta)\bar{q}_B^n(Q_F^2) + (A \leftrightarrow B)], \quad (14)$$

$$\begin{aligned} H_g^n(Q_F^2) &\equiv \sum_q e_q^2 [g_A^n(Q_F^2)(q_B^n(Q_F^2) + \bar{q}_B^n(Q_F^2)) \\ &\quad + (A \leftrightarrow B)]. \quad (15) \end{aligned}$$

The dependence on the azimuth is given by  $\Phi(\phi) = 1$  and  $\delta\Phi(\phi) = \cos 2\phi$ . Integration over  $\phi$  thus isolates the unpolarized part, and  $\Phi(\phi)$  is then replaced by  $2\pi$ . On the other hand the integration [20]

$$\left( \int_{-\pi/4}^{\pi/4} - \int_{\pi/4}^{3\pi/4} + \int_{3\pi/4}^{5\pi/4} - \int_{5\pi/4}^{7\pi/4} \right) d\phi$$

extracts the polarized cross section, and  $\delta\Phi(\phi)$  can then be simply substituted by 4. In the following we will always assume appropriate integration over the azimuth.

The unpolarized NLO  $\overline{\text{MS}}$  QCD coefficients in  $\tau$  space can be found, e.g., in Ref. [5]. Their Mellin moments are

$$\begin{aligned} C_q^{DY,n}(Q_F^2) &= C_F \left( 4S_1^2(n) - \frac{4}{n(n+1)} S_1(n) + \frac{2}{n^2} + \frac{2}{(n+1)^2} \right. \\ &\quad \left. - 8 + \frac{4\pi^2}{3} \right) + C_F \left[ \frac{2}{n(n+1)} + 3 \right. \\ &\quad \left. - 4S_1(n) \right] \ln \left( \frac{M^2}{Q_F^2} \right), \quad (16) \end{aligned}$$

$$\begin{aligned} C_g^{DY,n}(Q_F^2) &= T_R \left( -2 \frac{n^2+n+2}{n(n+1)(n+2)} S_1(n) \right. \\ &\quad \left. + \frac{n^4+11n^3+22n^2+14n+4}{n^2(n+1)^2(n+2)^2} \right) \\ &\quad + T_R \frac{n^2+n+2}{n(n+1)(n+2)} \ln \left( \frac{M^2}{Q_F^2} \right), \quad (17) \end{aligned}$$

where  $C_F = \frac{4}{3}$  and  $T_R = \frac{1}{2}$ . The polarized ones can be found in Ref. [8], and read

$$\begin{aligned} \delta C_q^{DY,n}(Q_F^2) &= C_F \left[ 4S_1^2(n) + 12[S_3(n) - \zeta(3)] + \frac{4}{n(n+1)} \right. \\ &\quad \left. - 8 + \frac{4\pi^2}{3} \right] + C_F [3 - 4S_1(n)] \ln \left( \frac{M^2}{Q_F^2} \right), \quad (18) \end{aligned}$$

$$\delta C_g^{DY,n}(Q_F^2) = 0. \quad (19)$$

In the above formulas we used the abbreviation  $S_k(n) = \sum_{j=1}^n j^{-k}$ . Since there is no gluon transversity distribution for the nucleon, the gluonic part of Eq. (13) drops out for the polarized case. The indices  $A$  and  $B$  in Eqs. (14) and (15) take into account the possibility of having two different scattering hadrons, although only  $pp$  collisions are planned at the moment. Finally,  $Q_F$  and  $Q_R$  in Eqs. (13)–(19) are the factorization and renormalization scales, respectively, for which we will choose  $Q_F = Q_R = M$  unless stated otherwise.

$Z^0$  production and  $\gamma Z^0$ -interference can be easily included by the substitution (see also Ref. [7])

$$\begin{aligned} e_q^2 \rightarrow e_q^2 - 8e_q V_l V_q \kappa \frac{M^2(M^2 - M_Z^2)}{(M^2 - M_Z^2)^2 + \Gamma_Z^2 M_Z^2} \\ + 16(V_l^2 + A_l^2)(V_q^2 \pm A_q^2) \kappa^2 \frac{M^4}{(M^2 - M_Z^2)^2 + \Gamma_Z^2 M_Z^2}, \quad (20) \end{aligned}$$

where

$$\kappa \equiv \frac{\sqrt{2} G_F M_Z^2}{16\pi\alpha_{em}}, \quad V_f \equiv T_f^3 - 2e_f \sin^2 \Theta_W, \quad A_f \equiv T_f^3. \quad (21)$$

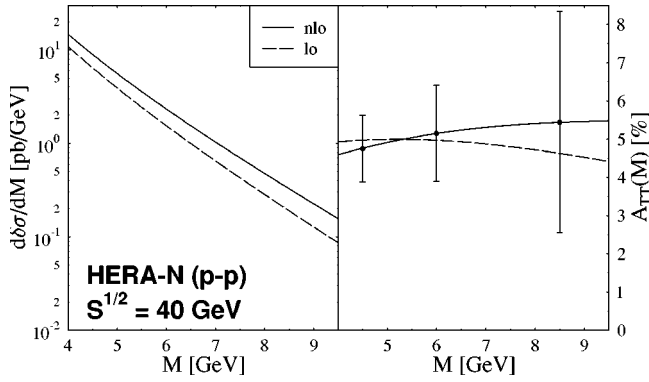


FIG. 3. NLO and LO maximal polarized Drell-Yan cross sections and asymmetries for HERA-N. The error bars were calculated according to Eq. (22), and are based on  $\mathcal{L}=240 \text{ pb}^{-1}$ , 70% polarization of the beam and target, and 100% detection efficiency.

The positive sign in front of the  $A_q^2$  term is appropriate for the unpolarized cross section, the negative sign for the polarized one. As usual,  $G_F$  denotes the Fermi constant,  $\Theta_W$  the Weinberg angle ( $\sin^2\Theta_W=0.224$ ), and  $T_f^3$  the third component of the weak isospin.

For examining the perturbative stability of our results, we will also calculate the cross section at LO. In this case one simply needs to set the QCD coefficients to zero in the above formulas, and to replace the NLO parton distributions by ones evolved in LO. As LO input distributions for Eq. (3), we will use the unpolarized LO parametrizations of Ref. [15] [neglecting again the SU(2) breaking in the quark sea] and the polarized ones of Ref. [16] at the LO input scale  $Q_0^2=0.23 \text{ GeV}^2$ .

#### IV. RESULTS

Figure 3 shows the transversely polarized  $pp$  cross section and the “maximal” double-spin asymmetry  $A_{TT}$  for  $\sqrt{S}=40 \text{ GeV}$ , corresponding to the proposed [21] HERA-N fixed target experiment which would utilize the possibly forthcoming polarized 820-GeV proton beam at the DESY  $ep$  collider HERA on a transversely polarized target. We show results at both LO and NLO. For illustration we have also included the expected statistical errors for a measurement of  $A_{TT}$  by HERA-N, which can be estimated from

$$\delta A_{TT} = \frac{1}{P_B P_T \sqrt{\mathcal{L} \sigma \epsilon}}, \quad (22)$$

where  $P_B$  and  $P_T$  are the beam and target polarizations, for which we will use  $P_B=P_T=0.7$ .  $\mathcal{L}$  is the anticipated integrated luminosity of  $\mathcal{L}=240 \text{ pb}^{-1}$ ,  $\sigma$  the unpolarized cross section integrated over bins of  $M$ , and  $\epsilon$  the detection efficiency for which we will take for simplicity  $\epsilon=100\%$ . Note that full  $4\pi$  coverage of the detector is assumed. Figure 3 shows that the maximal asymmetry for HERA-N is actually fairly large, and would be accessible in that experiment.

In Fig. 4 we present results similar to Fig. 3, but now for  $\sqrt{S}=150 \text{ GeV}$ , corresponding to the RHIC collider. We

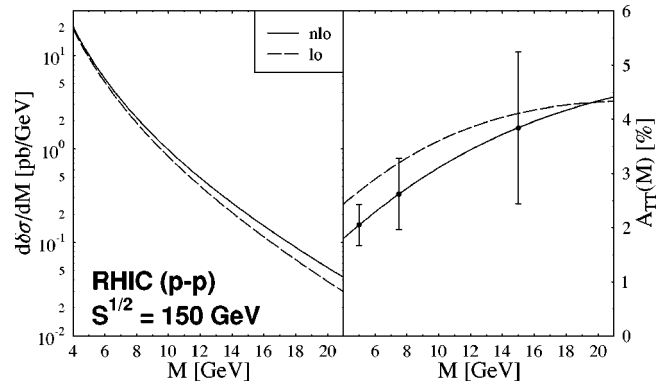


FIG. 4. As in Fig. 3, but for RHIC at  $\sqrt{S}=150 \text{ GeV}$  assuming  $\mathcal{L}=240 \text{ pb}^{-1}$ , 70% polarization of each beam, and 100% detection efficiency.

note that the region  $9 \text{ GeV} \lesssim M \lesssim 11 \text{ GeV}$  will presumably not be accessible experimentally, since it will be dominated by muon pairs from bottomonium decays. Again the predicted maximal asymmetry is of the order of a few percent. From the expected error bars calculated again for 70% beam polarization,  $\mathcal{L}=240 \text{ pb}^{-1}$  and  $\epsilon=100\%$ , one concludes that asymmetries of this size should be also well measurable at RHIC.

Figure 5 shows similar results for the high-energy end of RHIC,  $\sqrt{S}=500 \text{ GeV}$ , where the integrated luminosity is expected to be  $\mathcal{L}=800 \text{ pb}^{-1}$ . It turns out that the asymmetries become smaller as compared to the lower energies, but thanks to the higher luminosity the error bars become relatively smaller as well, at least in the region  $5 \text{ GeV} \lesssim M \lesssim 25 \text{ GeV}$ , where the errors are approximately  $\frac{1}{10}$  of the maximal asymmetry. One can also clearly see in Fig. 5 the effect of  $Z$  exchange and the  $Z$  resonance.

We have already mentioned before that Soffer’s inequation does not determine the sign of  $\delta q(x, Q^2)$ , so that in principle we have to check all different combinations in order to find the “true” maximal value for  $A_{TT}$ . It turns out, e.g., that keeping a positive sign only for  $\delta u_v(x, Q^2)$  leads to a reduction of  $|A_{TT}|$  at small  $M$ , but to an enhancement at the experimentally unaccessible region of large  $M$ . We have checked that for small  $M$  the asymmetry takes its largest values if all signs are chosen to be positive, as was done in Eq. (3) and in the above plots.

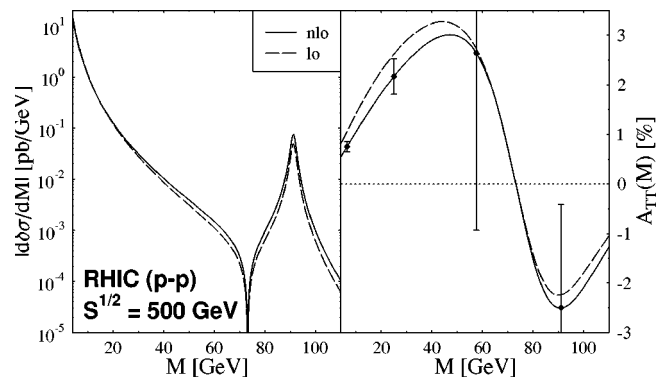


FIG. 5. As in Fig. 4, but for  $\sqrt{S}=500 \text{ GeV}$  and  $\mathcal{L}=800 \text{ pb}^{-1}$ .

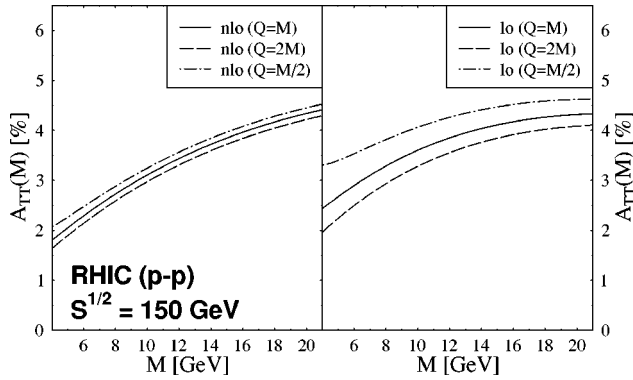


FIG. 6. Scale dependence of the LO and NLO asymmetries at  $\sqrt{S}=150$  GeV. The renormalization and factorization scales in Eqs. (13)–(15) were chosen to be  $Q_R=Q_F=M/2$ ,  $M$ , and  $2M$ . The solid line is as in Fig. 4.

A comparison of the LO and NLO results in Figs. 3–5 answers one key question concerning the transversely polarized Drell-Yan process: Our predictions for the maximal  $A_{TT}$  show good perturbative stability, i.e., the NLO corrections to the cross sections and  $A_{TT}$  are of moderate size, albeit not negligible. There seems to be a general tendency toward smaller corrections when the energy is increasing, which should be mainly due to the larger invariant masses probed and to a resulting smaller  $\alpha_s(M^2)$ .

Let us finally address some of the main uncertainties in our predictions for the maximal asymmetry  $A_{TT}$ . The first issue is the scale dependence of the results. This is examined in Fig. 6 for the case  $\sqrt{S}=150$  GeV. Here we plot the maximal asymmetry in LO and NLO, varying the renormalization and factorization scales in the range  $M/2 \leq Q_F = Q_R \leq 2M$ . One can see that already the LO asymmetry is fairly stable with respect to scale changes, which is in accordance with the finding of generally moderate NLO corrections. The NLO asymmetry even shows a significant improvement, so that  $A_{TT}$  becomes largely insensitive to the choice of scale.

In order to obtain a rough idea about the uncertainty caused by our imperfect knowledge of the longitudinally polarized parton densities  $\Delta q(x, Q^2)$  and  $\Delta g(x, Q^2)$ , we also calculated the asymmetries using the NLO “valence” scenario input distributions of [16] instead of the “standard” ones in Eq. (3). As can be seen in Fig. 7 for the case  $\sqrt{S}=150$  GeV, the difference for experimentally significant  $M$  turns out to be quite small, with the predictions based on the “valence” scenario distributions having slightly smaller asymmetries.

As we already mentioned in Sec. II, neither the “standard” nor the “valence” scenario parametrizations take into account a possible SU(2) breaking in the polarized sea because only neutral current polarized DIS data are available at the moment. This led us also to neglect any SU(2) breaking in the transversity input densities for our calculations, just keeping the dynamical SU(2) breaking produced by NLO evolution (cf. Fig. 2). On the other hand, it seems rather likely that a certain amount of SU(2) breaking — possibly

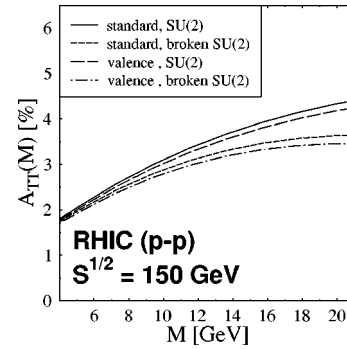


FIG. 7. The NLO asymmetry at  $\sqrt{S}=150$  GeV, using the “standard” and “valence” sets of Ref. [16] for the  $\Delta q(x, Q_0^2)$  in Eq. (3). Also shown is the change caused by not neglecting the SU(2) breaking in the  $q(x, Q_0^2)$  of Ref. [15] (see text). The solid line is as in Fig. 4.

much more than the one generated by evolution — could be realized in nature. One possible way of estimating the uncertainty entering our predictions for  $A_{TT}$  through this source, is to reintroduce the hitherto neglected amount of SU(2) breaking in the unpolarized input densities as fixed in the original input distributions of [15]. The SU(2) breaking will also influence the transversity input via Eq. (3). The resulting asymmetry is also depicted in Fig. 7. As can be seen, the effect is sizable only at rather large  $M$ .

## V. CONCLUSIONS

We have shown numerically that Soffer’s inequation is preserved by NLO QCD evolution, provided it is satisfied by the input distributions. For the first time, to our knowledge, we have presented a complete and consistent NLO calculation of the transverse double spin asymmetry  $A_{TT}$  for the Drell-Yan process, employing the NLO corrections to the hard subprocess cross sections as well as performing the  $Q^2$  evolutions in NLO. Here we have estimated the maximally possible  $A_{TT}$  in the framework of the radiative parton model by assuming that Soffer’s inequation is saturated at a low hadronic scale. For  $\sqrt{S}=40$  GeV the maximal value of  $A_{TT}$  for  $pp$  collisions was found to be approximately 4%, with an expected statistical error for HERA- $\vec{N}$  of about 1% at an invariant mass of  $M=4$  GeV. The situation for RHIC with  $\sqrt{S}=150$  GeV turned out to be rather similar. The prospects of measuring  $A_{TT}$  somewhat improved when going to  $\sqrt{S}=500$  GeV where the maximal asymmetry is of the order of 1% for small  $M$  with an expected relative statistical error of approximately 1/10. We emphasize again, however, that our results only represent an *upper bound* on  $A_{TT}$ , so that the “true” asymmetry may well be much smaller and even experimentally not measurable.

Comparing to corresponding LO calculations, we found that QCD corrections turn out to be moderate but non-negligible, putting our predictions on a firm basis. We have also examined the main uncertainties of our predictions, such as the scale dependence of the asymmetry and our imperfect

knowledge of the longitudinally polarized parton densities to be utilized for the saturation of Soffer's inequality at the input scale. We found that these uncertainties seem to have rather little impact on our results in the regions hopefully accessible in future experiments with transversely polarized protons.

*Note added.* After completing this work, we received Ref. [22], in which a mathematical proof of the preservation of Soffer's inequality under NLO  $Q^2$  evolution is given.

## ACKNOWLEDGMENTS

The work of M.S. was supported in part by the "Bundesministerium für Bildung, Wissenschaft, Forschung und Technologie" (BMBF), Bonn. O.M. and A.S. acknowledge financial support from the BMBF and the Deutsche Forschungsgemeinschaft. We thank G. Bunce for useful information concerning the RHIC luminosities. Furthermore, O.M. is grateful to T. Gehrman for helpful discussions and for providing an evolution program to crosscheck our results.

- 
- [1] J. P. Ralston and D. E. Soper, Nucl. Phys. **B152**, 109 (1979).  
 [2] R. L. Jaffe and X. Ji, Phys. Rev. Lett. **67**, 552 (1991); Nucl. Phys. **B375**, 527 (1992).  
 [3] X. Artru and M. Mekhfi, Z. Phys. C **45**, 669 (1990).  
 [4] RHIC Spin Collaboration, D. Hill *et al.*, letter of intent RHIC-SPIN-LOI-1991, updated 1993; G. Bunce *et al.*, Part. World **3**, 1 (1992); PHENIX/Spin Collaboration, K. Imai *et al.*, BNL-PROPOSAL-R5-ADD, 1994.  
 [5] See, e.g., W. Furmanski and R. Petronzio, Z. Phys. C **11**, 293 (1982).  
 [6] W. Vogelsang and A. Weber, Phys. Rev. D **48**, 2073 (1993).  
 [7] A. P. Contogouris, B. Kamal, and Z. Merebashvili, Phys. Lett. B **337**, 169 (1994).  
 [8] W. Vogelsang, Phys. Rev. D **57**, 1886 (1998).  
 [9] A. Hayashigaki, Y. Kanazawa, and Y. Koike, Phys. Rev. D **56**, 7350 (1997).  
 [10] S. Kumano and M. Miyama, Phys. Rev. D **56**, 2504 (1997).  
 [11] J. Soffer, Phys. Rev. Lett. **74**, 1292 (1995).  
 [12] V. Barone, Phys. Lett. B **409**, 499 (1997).  
 [13] X. Ji, Phys. Lett. B **284**, 137 (1992); R. L. Jaffe and N. Saito, *ibid.* **382**, 165 (1996); O. Martin and A. Schäfer, Z. Phys. A **358**, 429 (1997); V. Barone, T. Calarco, and A. Drago, Phys. Rev. D **56**, 527 (1997); S. Scopetta and V. Vento, FTUV-29, hep-ph/9706413; hep-ph/9707250.  
 [14] M. Glück, E. Reya, and A. Vogt, Z. Phys. C **48**, 471 (1990).  
 [15] M. Glück, E. Reya, and A. Vogt, Z. Phys. C **67**, 433 (1995).  
 [16] M. Glück, E. Reya, M. Stratmann, and W. Vogelsang, Phys. Rev. D **53**, 4775 (1996).  
 [17] R. L. Jaffe and A. Manohar, Phys. Lett. B **223**, 218 (1989); X. Ji, *ibid.* **289**, 137 (1992).  
 [18] D. A. Ross and C. T. Sachrajda, Nucl. Phys. **B149**, 497 (1979).  
 [19] M. Stratmann, W. Vogelsang, and A. Weber, Phys. Rev. D **53**, 138 (1996).  
 [20] J. L. Cortes, B. Pire, and J. P. Ralston, Z. Phys. C **55**, 409 (1992).  
 [21] V. A. Korotkov and W.-D. Nowak, Nucl. Phys. **A622**, 78c (1997).  
 [22] C. Bourrely, J. Soffer, and O. V. Teryaev, Phys. Lett. B. (to be published), CPT-97-P-3538, hep-ph/9710224.